Chapter 6

DNA & BSA binding, superoxide dismutation, antimicrobial activity and cytotoxicity of copper(II) containing metallogelator complexes

CHAPTER 6 DNA & BSA binding, superoxide dismutation, antimicrobial activity and cytotoxicity of copper(II) containing metallogelator complexes

6.1 BACKGROUND OF BIOLOGICAL STUDIES OF COMPLEXES

It was once said "The Biochemistry is coordination chemistry of living systems".[1] Now it is realized that in fact it is "the supramolecular chemistry of living systems", where the tertiary and quaternary assemblies of proteins have designated functions. Various metalloproteins play very important role in the routine biochemical processes.

With decades of dedicated work in the design and synthesis of novel supramolecular architectures, supramolecular synthesis of multi-functional systems has evolved and brought us closer to develop such systems for the betterment of mankind. If such kind of control is gained over the designing and interactions of the supramolecular assemblies, it would contribute to the development of biosensors, tissue engineering, host-guest assemblies, target selective drug delivery, etc.[2]

The coordination chemistry of bioactive molecules becomes important for their biological applications because the bioactive molecules choose and interact with the bioactive sites mainly through the supramolecular interactions and then the metal ions can further exert their effect through an associated redox, by inducing polarization and/or through template effect. Complexes of metal ions, especially, the biologically essential metal ions like copper have been reported to have good biological activities like DNA binding, BSA binding and antimicrobial activities. The metallogels reported in this thesis have been synthesized using metallogelator complexes involving copper(II) along with myo-inositol as the central moiety and bipy (chapter 2 and 4), phen and neocuproine (chapter 5) as capping ligands. Copper is a biologically essential metal ion, myo-inositol is a biomolecule and bipy, phen and neocuproine are all biologically benign molecules. Thus, they are expected to have significant biological activity. The ability of selected gels to interact with DNA, proteins, their ability to dismutate superoxide, antimicrobial activity and anticancer activity were investigated. These have been discussed in detail in the current chapter.

Materials and Instruments

The details of chemicals used and instruments used in all these studies are described below.

Materials

Ct-DNA, BSA, tris-buffer, ethidium bromide, NBT, PMS, β-NADH, sodium dihydrogen phosphate and disodium hydrogen orthophosphate (anhydrous) were procured from SRL for the DNA and BSA binding studies and for evaluating the superoxide dismutase activity. All these chemicals were used without any further purification. The metallogels 122, 131, 151, 132, 152, 133, 153, 231, 232, 251, 252 and 332 have been used for these studies. These were prepared as described in the earlier chapters (Ch.2, 4, 5).

UV-vis spectroscopy

UV-vis spectrophotometer was used to carry out studies of metal complexes and ligands. The spectrum was recorded using Perkin Elmer Lambda 35 dual beam UV-vis Spectrophotometer.

Fluorescence spectroscopy

Fluorescence spectra was recorded in solution phase on JASCO FP-6300 fluorescence spectrophotometer.

6.2 DNA binding

A variety of studies focusing on small molecules which react with the DNA strands via multiple non-covalent interactions (such as van der Waals interactions, H-bonding with the functional units bound along the groove of DNA helix and π-π interactions with the intercalation of aromatic heterocyclic groups between the base pairs) make them potential candidates for drug design.[3,4] Small molecules have the capability to stabilize the so-called adducts formed as they can conveniently bind with the DNA strands (via intercalation, insertion, groove binding and by discrete phosphate coordination, also called the 'phosphate clamp'[5]) without altering its configuration **(Figure 6.1.1)**. Transition metal complexes which form chelates are known for their potential to act as agents for probes of DNA structure in solution, mediation of strand scission, chemotherapeutic agents and so on. In this regard, transition metal complexes have proved to be a fascinating class as they exhibit well defined coordination geometries and very distinctive chemical, electrochemical and photo-physical properties which

enhance the functionality of the binding agents. It has also been established that such transition metal complexes have an intrinsic ability to bind to DNA.

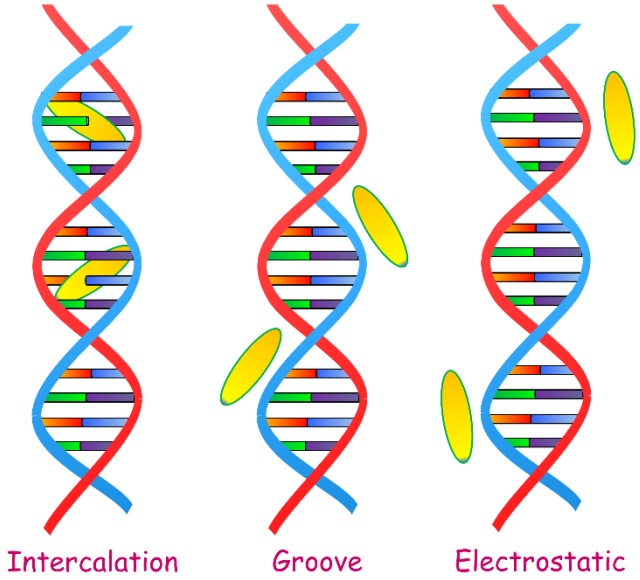

Figure 6.2.1 Possible modes of DNA binding

6.2.1 Experimental Procedures

Absorption Studies. The DNA binding studies were performed in tris(hydroxymethyl)-aminomethane-HCl (15 mM)/NaCl (150 mM) buffer (pH adjusted to 7.5 with conc. HCl) using 1 mM solutions of complexes prepared in DMSO. The concentration of calf thymus-DNA (solution prepared in TRIS-HCl/NaCl buffer) was acquired from absorption intensity observed at 258 nm using molar extinction coefficient value of 6600 M^{-1}. The absorption titration experiments were performed with a fixed concentration of metallogelator complex in the cuvette and gradually increasing the concentration of DNA in the cuvettes. An equal amount of DNA was added to both the cuvettes, containing the test solution and the reference in order to eliminate the absorbance of DNA itself. The ratio of the concentration of DNA: metallogelator complex has been mentioned in each of the cases, in the graphs represented in the **Figure 6.2.2.1.**

Ethidium Bromide Displacement Assay*:* For emission studies, a solution containing DNA and 166.67 μM EB in TRIS-HCl/NaCl buffer was titrated by addition of complexes at RT (313 K). The influence of complexes on DNA-EB was recorded with λ_{ex} = 546 nm and λ_{em} = 610 nm, at a bandwidth of 2.5 nm. The fluorescence titration experiments were performed with a fixed concentration of DNA in the cuvette and gradually increasing the concentration of metallogelator complex. The ratio of the

concentration of metallogelator: DNA complex has been mentioned in each of the cases, in the graphs represented in the **Figure 6.2.2.3.**

6.2.2 Results and Discussion

DNA binding studies using UV-Visible absorption spectra

The ability of metal complexes to bind with DNA can be studied by absorption titration. Generally, a metal complex having an aromatic backbone binds with DNA causing a change in absorption (hypochromism in intercalative mode and hyperchromism in groove binding) and bathochromism (shift in wavelength) as a result of strong stacking interactions between the complex and base pairs of DNA.

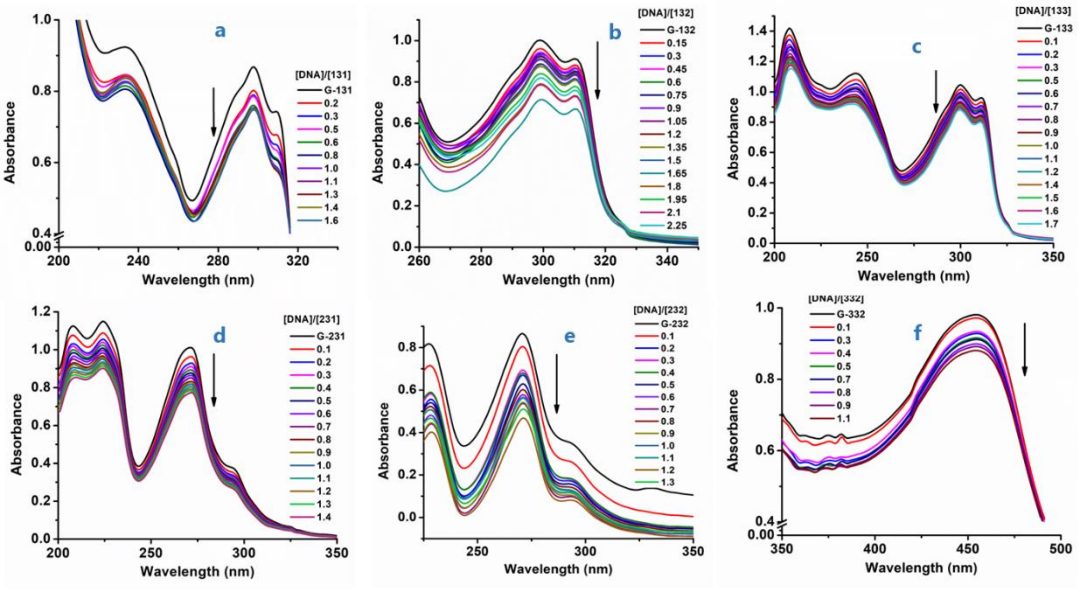

Figure 6.2.2.1 (a) Absorption titration spectra of (a) **131** (b) **132** (c) **133** (d) **231** (e) **232** and (f) **332** in absence and presence of ct-DNA at 30°C in 15 mM Tris-HCl/150 mM NaCl buffer (pH=7.5). The downward arrow shows a decrease in absorption intensity with increasing DNA concentrations.

It can be seen that the absorption band around 450 for metallogelator complex 332 and 270 nm for rest of the complexes (caused by π-π* transition) suffered a significant hypochromism **(Figures 6.2.2.1).** These results are indicative of the fact that the metallogelator complexes could bind to DNA via intercalative mode.

The intrinsic binding constant, K_b was determined using Mehan's equation[6]:

$$[DNA] / (\varepsilon_A - \varepsilon_F) = [DNA] / (\varepsilon_b - \varepsilon_F) + 1 / K_b (\varepsilon_b - \varepsilon_F)$$

where [DNA]= concentration of DNA in base pairs, $\varepsilon_A = A_{obsd}/[compound]$, ε_F = extinction coefficient for unbound compound, ε_b = extinction coefficient for compound

in fully bound form. The plot of [DNA]/(ε_A-ε_F) vs. [DNA] **(Figures 6.2.2.2)** gave a slope 1/(ε_b-ε_F) and an intercept of 1/K_b(ε_b-ε_F).

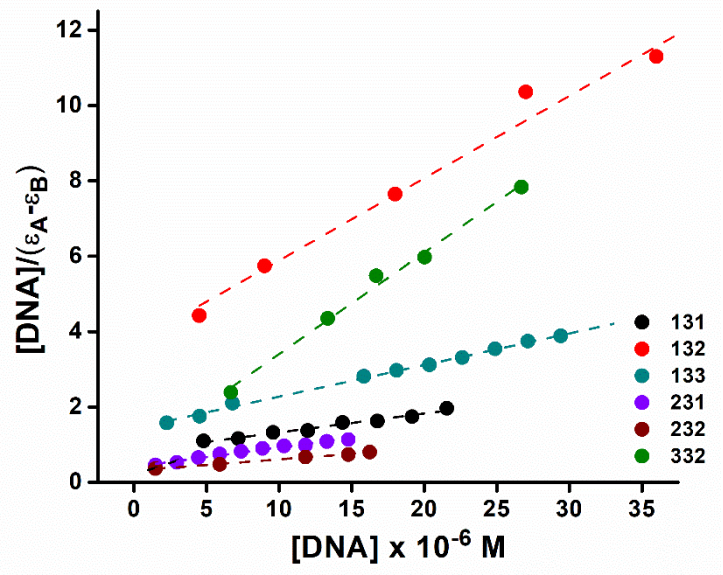

Figure 6.2.2.2 Plots of [DNA]/(ε_A-ε_F) vs. [DNA] for all metallogelator complexes.

It is known that shape, size, hydrophobicity and electrolytic behavior of the complexes play a vital role in their interactions with DNA. Higher K_b values for **332** suggests that the more aromatic ligands contribute to a stronger affinity, and hence, better binding ability with ct-DNA.

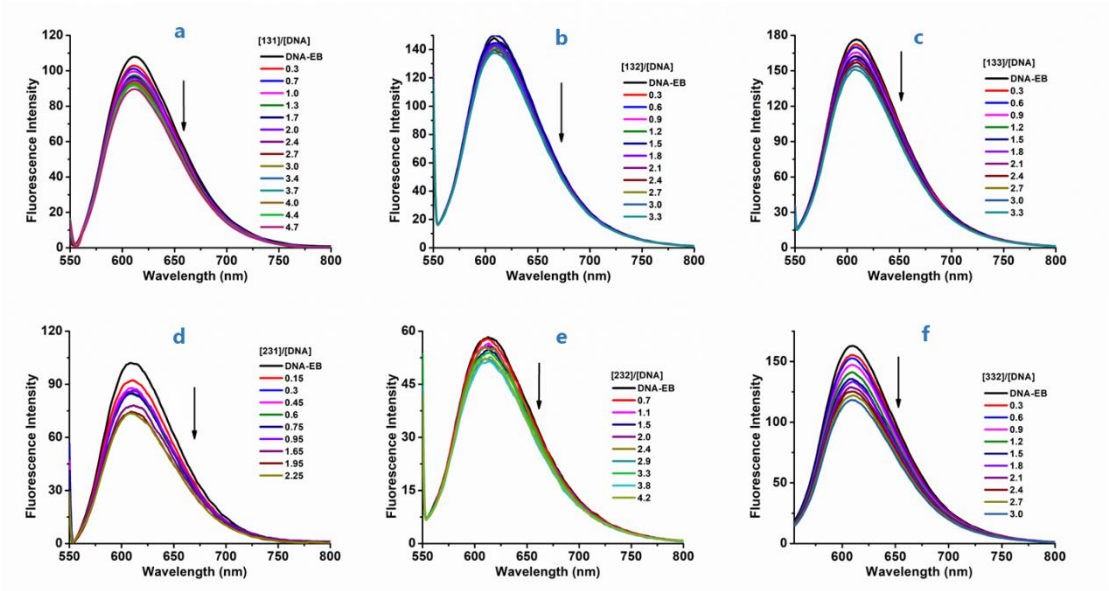

Figure 6.2.2.3 Emission spectra of EB bound to DNA in presence of metallogelator complexes (a) **131,** (b) **132,** (c) **133** (d) **231** (e) **232** and (f) **332.**

DNA Binding studies using Fluorescence measurements

Ethidium Bromide (EB) displacement assay was also performed by fluorescence spectral titration technique for the metallogelator complexes. The titration plots are displayed in **Figures 6.2.2.3.** Addition of metallogelator complexes is accompanied by a quenching in the fluorescence intensity of DNA-EB. It shows that the complexes can fairly bind to ct-DNA, releasing the already bound EB. The quenching constant, K_{SV} of the compounds was determined from the Stern-Volmer equation:

$$\mathbf{I_0/I = 1 + K_{SV}\,[Q]}$$

K_{SV} was obtained from the slope of the plot of I_0/I vs. [Q] **(Figure 6.2.5)** and the values are listed in **Table 6.2.2.1.**

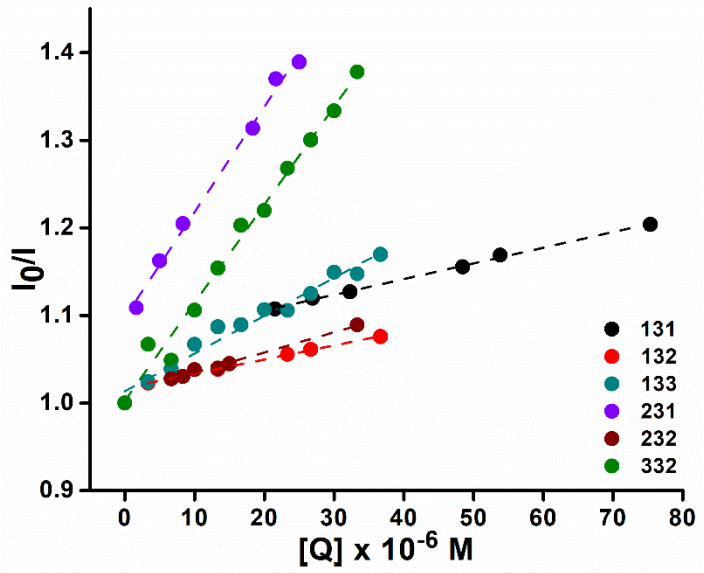

Figure 6.2.2.4 Stern-Volmer plots of emission intensity I_0/I vs. [Q]

Table 6.2.2.1 DNA binding values/interactions for metallogelator complexes

Codes	K_{sv} (10^3 M^{-1})	K_b (10^5 M^{-1})
131	1.9	1.5
132	1.727	0.58
133	5.77	0.57
231	16.9	1.2
232	1.665	0.93
332	13.376	3.7

From the UV plots it is found that the values follow the order **332 > > 131 >231 > 232 > 132 > 133** and fall in the magnitude of $\mathbf{10^4/10^5\ M^{-1}}$, which suggests that the complexes interact with DNA strongly. Also, the interaction of **332** with DNA is strongest, which is validated by absorption results.

The metallogelator complex **332, 231/232, 131/132/133** differ in the presence of capping ligands, i.e., neocuproine, phen and bipy, respectively. It was observed in general that as the aromatic character of the ligands increases it facilitates the binding of the metallogelator complex with DNA. As the metallogelator complexes bind with DNA through intercalative mode, ligands like phenanthroline and neocuproine when used as capping agents increase the chances of binding with DNA. This can be seen in the results tabulated in the **Table 6.2.2.1.**

The fluorescence spectral titrations carried out using EB caused a quenching in the fluorescence intensity of DNA-EB complex on gradual addition of complexes. The fluorescence data also indicates that the metallogelator complexes **231** and **332** containing phen and neocuproine, respectively, as capping agent binds to the DNA fairly strongly, again asserting the fact that increase in the organic backbone of the molecule facilitates DNA binding through intercalation mode. Other metallogelator complexes also bind to the DNA fairly strongly. The binding constant have been documented in the **Table 6.2.2.1.** The K_{SV} values which are an indication of DNA binding strength calculated from fluorescence spectroscopic data are of the magnitude of $\mathbf{10^3/10^4\ M^{-1}}$**.**

6.3 Interactions with Protein

Serum albumins are the most soluble proteins found in mammalian blood plasma and play an important role in many physiological functions. They are also involved in transportation, distribution and metabolism of drugs, amino acids and metal ions. Investigation of binding mechanism of drugs with serum albumins is very important as it influences the absorption, distribution, metabolism and excretion of the drugs. In that regard, Bovine Serum Albumin (BSA) is most commonly used as relevant models for establishing the affinity of small molecules with albumins. It is widely available, inexpensive and structurally resembles Human Serum Albumin (HSA) by approx. 76%.[7,8]

BSA is a globular, non-glycosylated protein, made of 583 amino acid residues which are bound in a single chain and crosslinked via 17 cysteine residues (eight disulfide bonds and one free thiol group), with a molecular mass of 66400 Da. The high solubility of BSA arises from the presence of ionized residues, such as glutamic acid and lysine and variable content of tryptophan, methionine, isoleucine, etc. These ionized residues confer the protein with a high charge, of 185 ions/molecule at a neutral pH.[8]

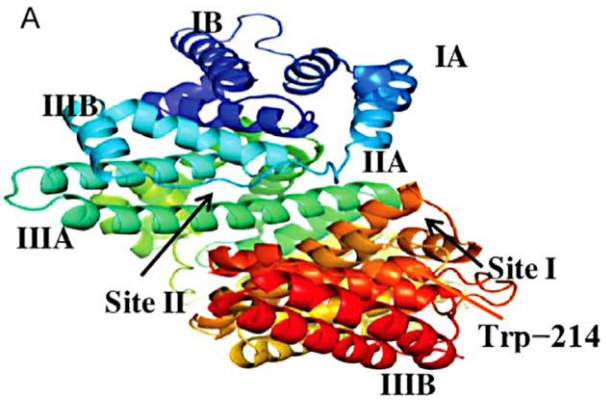

Figure 6.3.1 Discrete binding sites of BSA protein

6.3.1 Experimental Procedure

The interaction with protein was studied using fluorescence quenching experiments in bovine serum albumin stock solution (BSA, 16.67 μM) in tris(hydroxymethyl)-aminomethane-HCl (15 mM)/NaCl (150 mM) buffer (pH adjusted to 7.5 with conc. HCl). The spectra were recorded at RT (313 K) with λ_{ex} = 296 nm and λ_{em} = 344 nm. The concentration of BSA was kept constant and the complex concentration was raised, systematically. Synchronous fluorescence spectra of BSA in presence of metallogelator complexes was also recorded using the same concentrations at two different Δλ values (difference between excitation and emission wavelengths of BSA) of 15 and 60 nm.

6.3.2 Results and Discussion

Fluorescence spectral titration technique is used in order to investigate the ability of the molecules to bind with BSA. Conformational and dynamic changes in the protein structure are indicated by the quenching in the fluorescence intensity of BSA, also accompanied by a blue shift.[9] Tryptophan (Trp) and tyrosine (Tyr) residues present in the structure of the BSA are responsible for the fluorescent behavior of BSA. The intensity of the fluorescence of the BSA decreases with increasing concentrations of all the metallogelator complexes as shown in **Figure 6.3.2.1.**

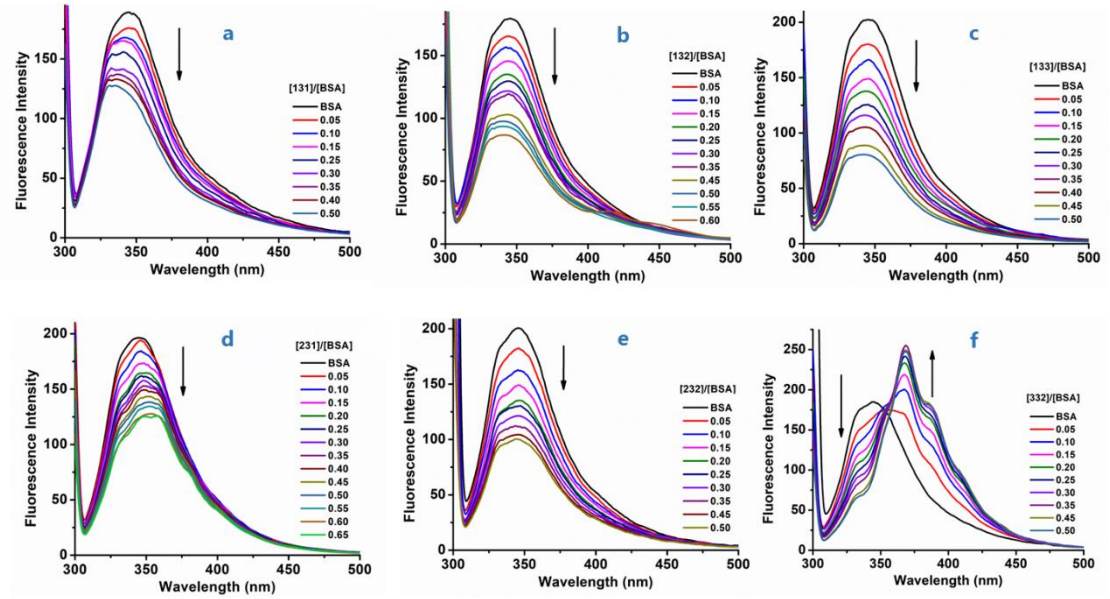

Figure 6.3.2.1 The emission spectra of BSA (16.67 x 10-6 M; λ_{ex} = 296 nm, λ_{em} = 344 nm) in presence of increasing amounts of (a) **131**, (b) **132**, (c) **133** (d) **231** (e) **232** and (f) **332.**

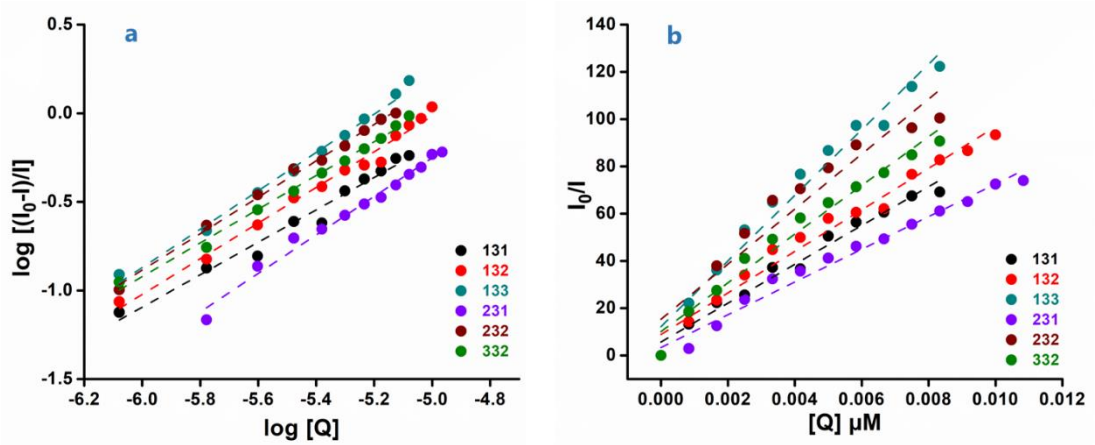

Figure 6.3.2.2 Figure showing (a) Scatchard plots and (b) Stern-Volmer plots of fluorescence quenching with different concentrations of metallogelator complexes.

The Stern-Volmer equation[10] was used to calculate the fluorescence quenching constant, Stern-Volmer constant K_{SV}:

$$\mathbf{I_0 / I = 1 + K_{SV}\,[Q]}$$

where I_0 and I are the fluorescence emission intensities in the absence and presence of a quencher (complex) respectively and [Q] is the concentration of quencher (metallogelator complex); K_{SV} was obtained from the slope of the plot of I_0/I vs. [Q] **[Figures 6.3.2.2 (b)]**.

The addition of metallogelator complexes cause quenching of fluorescence which proves the interaction between metallogelator complexes and the BSA protein. The

binding constants of the metallogelator complexes with BSA protein were calculated according to Scatchard equation[11]:

$$\log [(I_0 - I) / I] = \log K_{BSA} + n \log [Q]$$

where K_{BSA} is the binding constant of complexes with BSA (calculated from the intercept of plots of log[(I_0–I)/I) and log[Q] (**Figures 6.3.2.2 (a))** and *n*, the number of binding sites, obtained from the slope value. The *n* values for **all the metallogelator complexes** are close to **1**, which is suggestive of the presence of a single binding site in the BSA protein structure. However, the K_{BSA} values follow the order **133 > 232> 332 > 132 > 131 > 231**, again revealing the fact that metallogelator complexes having neocuproine and phenanthroline as capping ligands have good interaction with BSA. It was also observed that the metallogelator complex **133** having bipy as capping ligand has the highest binding capacity with BSA.

The following equation was used to determine the bimolecular quenching rate constant K_q:

$$K_q = K_{SV} / \tau_0$$

where K_{SV} is the Stern-Volmer constant and τ_0 is the average lifetime of the fluorophore in the absence of the quencher (τ_0 = 10 ns for BSA[12]).

Table 6.3.2.1 BSA binding parameters of the metallogelator complexes

Codes	K_{sv} (10^5 M^{-1})	K_q (10^{13} $M^{-1}s^{-1}$)	K_{BSA} (10^5 M^{-1})	n
131	**0.708**	**0.708**	**0.2498**	**0.9153**
132	**0.944**	**0.944**	**1.035**	**1.0062**
133	**1.615**	**1.615**	**4.198**	**1.08**
231	**0.546**	**0.546**	**22**	**1.3112**
232	**1.308**	**1.308**	**1.1**	**0.9859**
332	**1.11**	**1.11**	**0.609**	**0.9511**

It appears that the interaction with the protein is mainly through ligands and the extent of binding varied depending on the balance between the σ- and π-interaction with the metal ion in the complexes which affects the electron density over the ligands through polarization.

The values of quenching constants for the binding of BSA to the compounds are of the order $10^{12/13}$ $Lmol^{-1}s^{-1}$, which are two/three-fold higher than the maximum scatter collision quenching constant of BSA, 2.0 x 10^{10} $Lmol^{-1}s^{-1}$.[12] This means that the quenching of BSA fluorescence by the metallogelator complexes is not initiated by a dynamic mechanism. Also, the double logarithmic Scatchard plots for all metallogelator complexes were found to be straight lines as indicated in the **Figure 6.3.2.2 (a)**, which suggests that the quenching is caused by the formation of a complex, indicating a static quenching mechanism.

6.3.2.1 BSA conformational analysis

In order to get an information about the molecular microenvironment in the vicinity of the fluorophores, synchronous fluorescence spectra of BSA were recorded in presence of the synthesized metallogelator complexes.

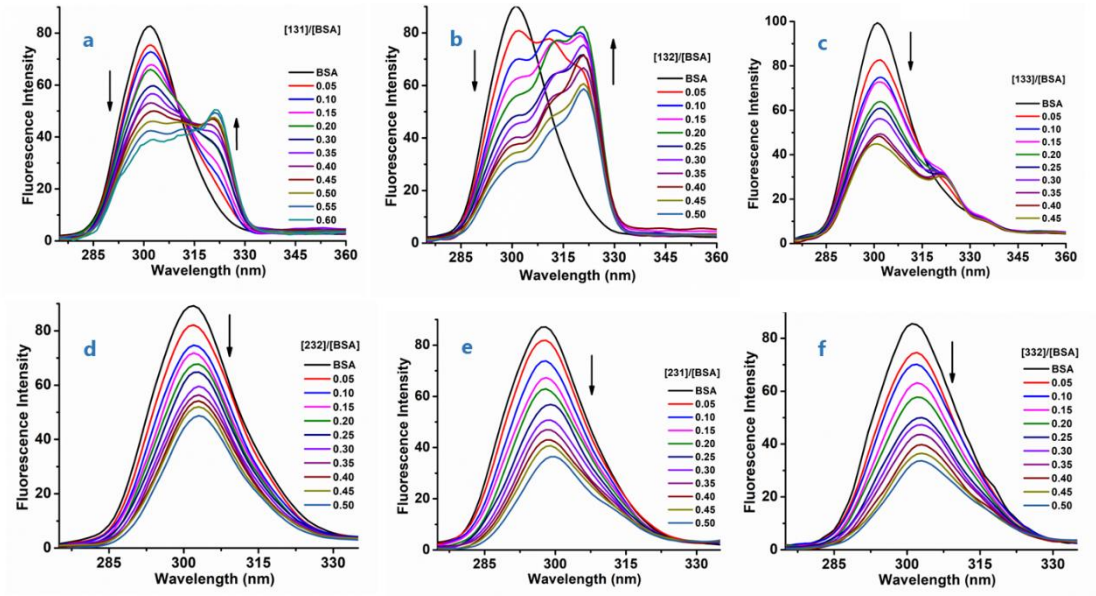

Figure 6.3.2.3 Synchronous BSA spectra in tris-HCl/NaCl buffer (pH=7.5) in presence of increasing concentrations of **131** (a), **132** (b), **133** (c), **231** (d), **232** (e) and **332** (f) at **Δλ =15 nm** (the downward arrow signifies a decrease in fluorescence intensity with increasing concentration of quencher).

This study can indicate the possibility of binding with different aminoacid residues in the proteins when the spectra are recorded at different Δλ values corresponding to different nature of chromophores; for a Δλ value of 15 nm, the fluorescence of BSA is characteristic of tyrosine residue, while a Δλ value of 60 nm, it corresponds to the tryptophan residue.[13,14]

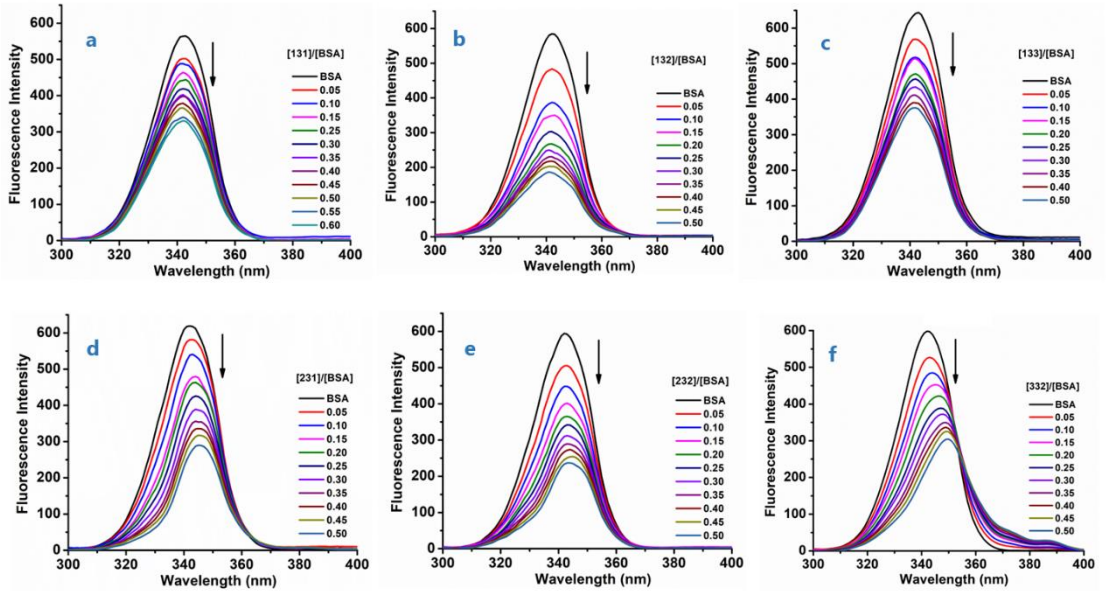

Figure 6.3.2.4 Synchronous BSA spectra in tris-HCl/NaCl buffer (pH=7.5) in presence of increasing concentrations of **131** (a), **132** (b), **133** (c), **231** (d), **232** (e) and **332** (f) at **Δλ =60 nm** (the downward arrow signifies a decrease in fluorescence intensity with increasing concentration of quencher).

The quenching of BSA fluorescence was monitored through a simultaneous scanning at wavelength difference of 15 nm and 60 nm. The synchronous BSA spectra for various concentrations of complexes at Δλ =15nm **(Figure 6.3.2.3)** shows a decrease in the fluorescence intensity at 300 nm with a minor shift of 0-10 nm. The decrease in fluorescence intensity as compared to the initial values was observed to be ~ **45 %** for **232**, **~ 55-60%** for **131**, **133**, **231** and **332** while the decrease in fluorescence intensity was upto **~ 70%** for **132.**

The spectra at Δλ = 60 nm **(Figure 6.3.2.4)** for increasing concentrations of complexes also showed a regular and significant decrease in the intensity at 341 nm, upto ~ **40 %** of the initial fluorescence intensity of BSA for metallogelator complexes **131** and **133** and **~ 50-60%** for **231, 232** and **332** while the decrease in fluorescence intensity was upto **~ 70%** for **132**. These results clearly suggests that all complexes interact with both Tyr and Trp residues.

6.4 Dismutation of superoxide ion

The superoxide ion is a product of oxygen metabolism in the living systems and can be a mediator of reperfusion diseases such as myocardial infarction (stroke), initiate inflammatory processes associated with diseases like arthritis, even cause oxidative

injury to the tissues which can lead to various neurological disorders like Parkinson's and Alzheimer's diseases.[15]

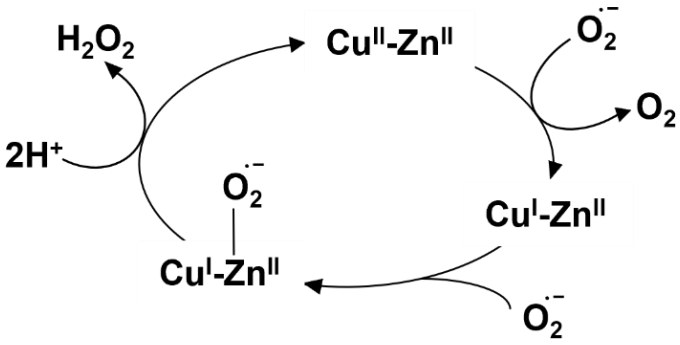

Scheme 6.4.1 Catalytic cycle in a conventional SOD complex

Naturally occurring superoxide dismutases (SOD) in living systems contain Cu/Zn and Mn centers, which act as a natural defense mechanism against the superoxide-mediated oxidative damages in the cells.[16,17] The catalytic cycle of a conventional SOD follows a 'ping-pong' mechanism, where disproportionation of two superoxide anions ($O_2^{\bullet-}$) results in the formation of molecular oxygen (O_2) and hydrogen peroxide (H_2O_2), as shown in **Scheme 6.4.1.**

It has been long known that redox-active transition metal ions in a coordination environment make good candidates for biological catalytic activity in redox reactions.[18] Specially, those containing copper(II) have redox potentials matching with reactive oxygen species and hence they can be best utilized in catalyzing the dismutation of superoxide anion.

Synthetic enzymes (*synzymes*) which can mimic a natural enzyme function carry a potential to act as pharmaceutical agents for the treatment of aforementioned neuro-degenerative disorders and may possess superior anticancer activity. In this regard, low molecular weight SOD mimics are of prime importance as they have the ability to access intercellular space, have cellular permeability, longer half-life in the blood, potential for oral delivery, etc. and naturally, umpteen SOD mimicking complexes have been prepared and reported in the literature.[17,19,20] Most commonly employed complexes possess either mono/bi-nuclear Cu^{2+} and/or Zn^{2+} centers. This inspired us to exploit the abilities of the synthesized copper(II) complex gelators to act as SOD *synzymes*. The study has been further extended to assess the DNA cleavage ability of all the ligands and complexes.

6.4.1 Experimental Procedures

Antioxidant assay

The superoxide dismutase (SOD) activity was measured using NADH-PMS-NBT method **(Scheme 6.4.1.1)**.[21] Non-enzymatic (β-NADH-PMS-NBT) system containing 30 μM PMS and 80 μM NADH in phosphate buffer(pH=7.8) at RT (313 K) was used to produce superoxide ion which reacted with 75 μM NBT to form bluish-black colored formazan complex. The absorbance of the solutions was monitored at 560.0 nm at various concentrations of the complexes under uniform conditions in triplicates.

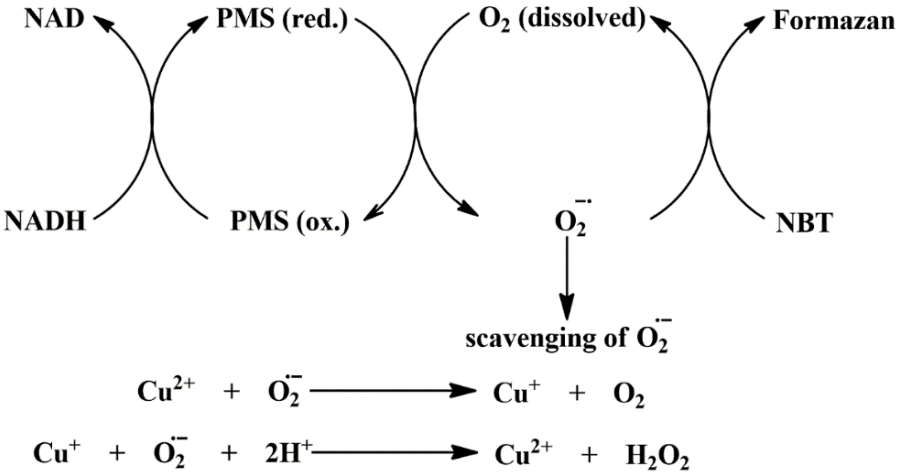

Scheme 6.4.1.1 Assessing SOD mimic activity using β-NADH-PMS-NBT method

The % inhibition of NBT reduction was calculated using the following equation:

% inhibition of NBT reduction = **(1-(k'/k))*100 %**

where k, k'= slope of the straight line obtained from absorbance values as a function of time in absence and presence of complex. The IC_{50} value was calculated as the concentration of the complex that caused 50% inhibition of NBT reduction, from the plots of % inhibition vs. concentration of complex (μM).

6.4.2 Results and discussion

As mentioned above, copper(II) is present at the active site of the superoxide dismutases (SOD). Various copper(II) complexes are known to show good superoxide dismutase activity. The trinuclear metallogelator complex yielding metallogels have copper(II) as the metal center, due to which they were expected to possess superoxide dismutase (SOD) activity.

Table 6.4.2.1 IC_{50} values for the synthesized complexes and similar Cu complexes reported in literature		
Complex	**IC_{50} (µM)**	**Reference**
131 [a]	**2.9**	**Present work**
132 [a]	**0.8**	
133 [a]	**0.54**	
151 [a]	**1.02**	
152 [a]	**0.45**	
153 [a]	**0.37**	
231	**6.62**	
232	**6.35**	
251	**4.23**	
252	**6.04**	
332	**4.34**	
Native Cu-Zn SOD [b]	0.03-0.15	22,23
Vitamin C [a]	852	24
$Cu(en)_2Cl$ [a]	1000	22
$CuCl_2.2H_2O$ [b]	0.910	25
$CuSO_4$ [b]	30.0	26
$[Cu_2(indo)_4(H_2O)_2]$ [c]	1.31	26
Cu(II) salan complexes [b]	0.75-3.0	27
[Cu(sal)(phen)] [b]	1.01	26

***(IC_{50} was determined by a= inhibition of NBT, b= xanthine/xanthine oxidase, c= alkaline DMSO)**

The complexes reported here have been found to be active SOD mimics, being able to scavenge the superoxide at low concentrations. The IC_{50} values obtained from the above experiments are listed in **Table 6.4.2.1**, along with those of native Cu-Zn SOD and certain selected compounds from the literature. It is remarkable that the IC_{50} values for the complexes fall in the range of **0.37-2.9 µM**, in the order, **153 > 152 > 133 > 132 >151 >131**. We can infer that the synthesized complexes are more efficient than Vitamin C, $CuSO_4$, $Cu(en)_2$ and number of previously reported SOD mimics in literature. All the copper(II) metallogelator complexes synthesized turned out to be catalytically active SOD mimics, being able to scavenge the superoxide at exceptionally low concentrations.

The IC_{50} values of the metallogels depend on the counter anion and the base used for gelation. In the metallogelator series having 2,2'-bipyridine as the capping ligands it was observed that the increase in the chain length of carbon atoms in the carboxylate counter anion is accompanied by a decrease of IC_{50} value. The IC_{50} values of metallogelator complexes decrease in the order **131 > 132 > 133**, i.e., the SOD activity increases in the order **133 > 132 > 131** as the length of the alkyl chain increases. Further it was also observed that when the alkyl chain length is kept constant, the alkali used also affects the IC_{50} values. When the gels were synthesized in presence of sodium carbonate, they had lower IC_{50} values and higher activity as compared to the counterparts synthesized using potassium carbonate. This proves that even the slightest changes in ligand design and coordination environment of a complex or the changes in the medium can substantially affect the activity of the complexes.

On the contrary when the capping ligand was changed to 1,10-phenanthroline or neocuproine the IC_{50} values of the metallogelator complexes were found to increase drastically as compared to their bipy analogues. Further it was also observed that the change in anion or the type of carbonate base used doesn't significantly affect the IC_{50} values of these metallogelator complexes. The IC_{50} values were found to fall in the range of **(4.34-6.62μM, Table 6.4.2.1)** when phen or neocuproine was used as a capping ligand.

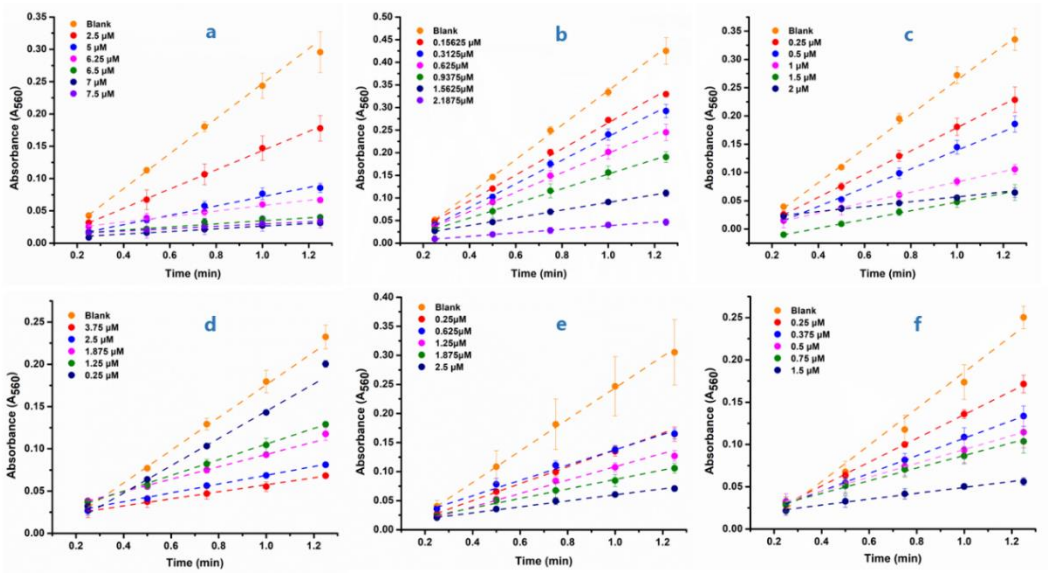

Figure 6.4.2.1 Plots of absorbane A_{560} as a function of time of the metallogelator complexes **131** (a), **132** (b), **133** (c), **151** (d), **152** (e), **153** (f).

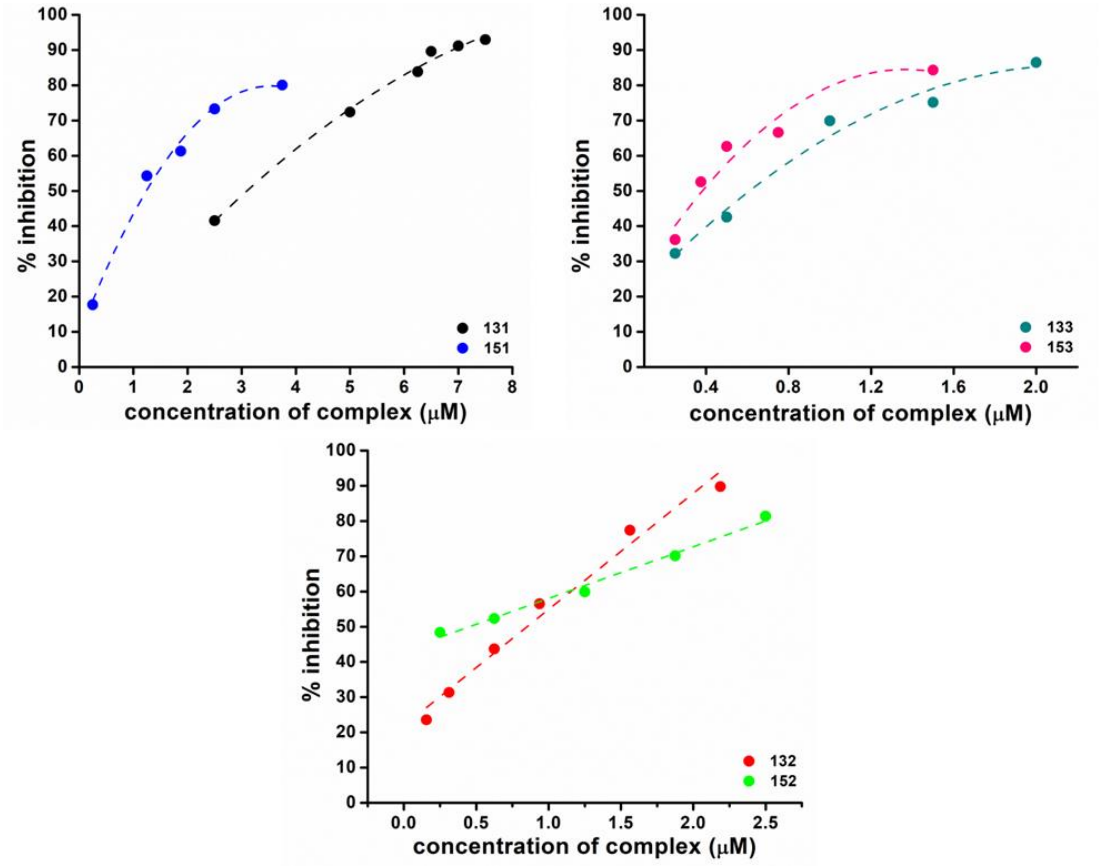

Figure 6.4.2.2 Plot of % inhibition as a function of [metallogelator complex] of complexes **131, 132, 133, 151, 152** and **153.**

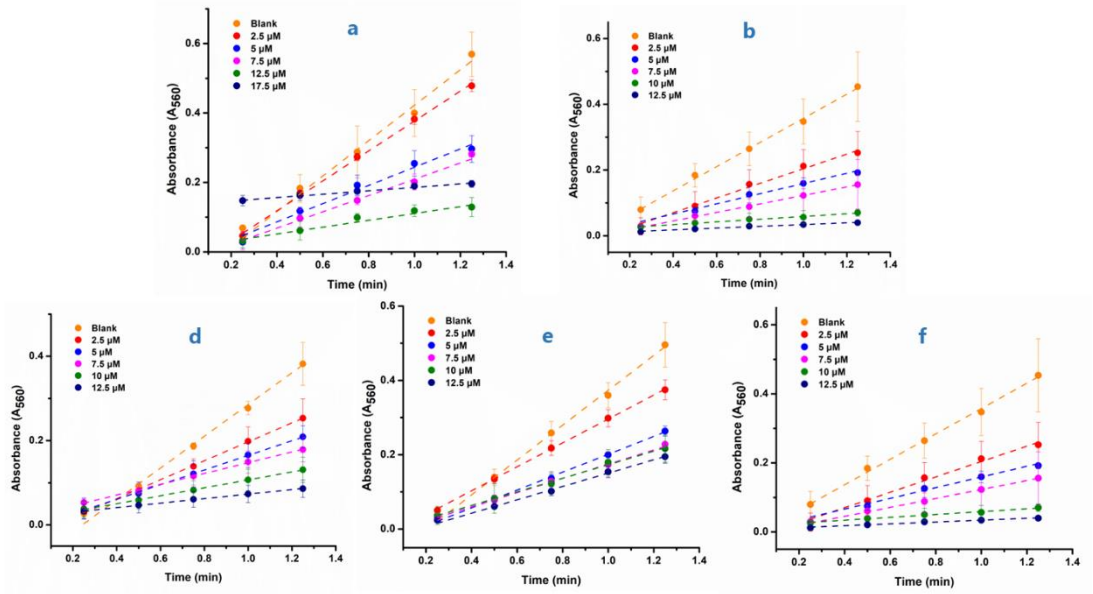

Figure 6.4.2.3 Plot of absorbane A_{560} as a function of time of the metallogelator complexes **231** (a), **232** (b), **251** (c), **252** (d), **332** (e).

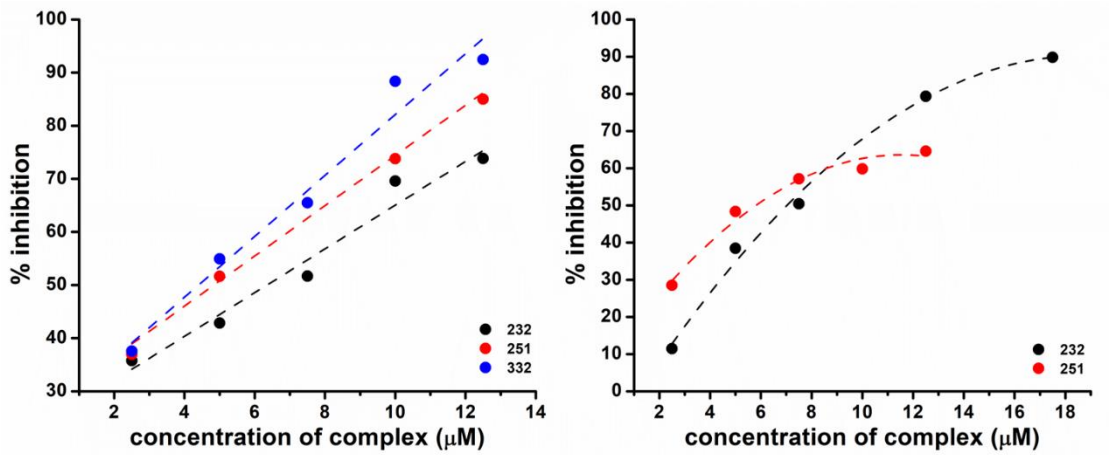

Figure 6.4.2.4 Plot of % inhibition as a function of [metallogelator complex] of complexes **231, 232, 251, 252** and **332**.

6.5 Cytotoxicity on Human Hepatoma (HepG2) cell line

In spite of so much advancement in the field of modern science and medicine, cancer, unfortunately remains one of the deadliest diseases of the modern world and is one of humanity's greatest health challenges today. Cancer is responsible for the second highest deaths on account of diseases globally, just behind cardiovascular diseases. According to WHO estimates, the number of deaths due to cancer is expected to increase to over 14.5 million by 2035.[28,29] In 1960, a big milestone for anticancer drug application in medicine was achieved by the discovery of platinum's inhibitory effect on tumor cell growth.[30,31] Cisplatin was one of the first anticancer platinum(II) compound which has platinum(II) metal at the center of the square planar structure and is coordinated with two chlorides and two ammonia molecules in a cis configuration. After the discovery of cisplatin, many cisplatin analogous drugs (carboplatin of second generation and oxaliplatin of third generation) were discovered and are used worldwide in clinical applications and several other platinum analogs (lobaplatin, nedaplatin, and heptaplatin) are approved in several countries.[32] However, the use of these anticancer platinum containing drugs is limited to an extent due to the serious side effects of these drugs which include toxicities on the kidney, heart, ear and liver, decrease in immunity, hemorrhage, and gastrointestinal disorders.[33–35] Due to these limitations of platinum based anticancer compounds, researchers are accelerating their efforts to discover and design new anticancer compounds in the war against cancer. In today's critical situation, there is an urgent need to replace current drugs with appropriate alternatives to resolve the current limitations. Several transition metals from the d-block of the periodic table

(groups 3 to 12) and particularly biologically essential trace metals,[36,37] such as copper,[38–41] are considered useful for the implementation of metal-based complexes in anticancer therapies. Specially, the presence of copper is anticipated to be beneficial since it has an ability to oxidatively cleave the DNA of cancer cells. The metallogels reported in this thesis are complexes containing copper(II) ions and hence it was thought to be worth exploring the anticancer properties of these compounds. In order to explore these properties, cytotoxicity studies were performed on human hepatoma cancer cell line. The metallogels are synthesized by a trinuclear copper(II) complex which has organic molecules like bipy, phen or neocuproine as capping ligands and myo-inositol as a central moiety. All these molecules are benign and it is expected that the supramolecular framework that is formed with these nontoxic moieties also would be harmless to healthy living cells. Few of the metallogels – **132, 232** and **332** having bipy, phen and neocuproine, respectively, and were synthesized at near physiological pH using carbonate bases were selected as representative compounds to carry out MTT assay, the results of which are discussed here.

6.5.1 Experimental Procedures

6.5.1.1 Materials and Methods

Human Hepatoma (HepG2) cells were procured from National Centre for Cell Science (NCCS, Pune, India).

6.5.1.2 MTT assay

Human Hepatoma (HepG2) cells were procured from National Centre for Cell Science (NCCS, Pune, India). Cells were cultured in T25 flasks in complete DMEM growth media, supplemented with 10% FBS and 1% antibiotic antimycotic solution. The cells were incubated in 5% CO_2 at 37°C temperature in CO_2 incubator (Thermo scientific, forma series II 3110, USA). Cell passaging was at 80% confluency using 1X TPVG (Himedia, India). For cytotoxic assessment, an MTT assay was performed. MTT assay is dependent on mitochondrial respiration and indicated a number of viable cells in the system. HepG2 cells ($8x10^3$ cells/well) were seeded in 96 well plates in a complete DMEM growth medium. After 24h of seeding the plate was used for dosing of different target compounds. The target compounds were dissolved and prepared in an incomplete media with desired concentrations. Cells were incubated with the test compounds for 24h. Following 24h of dosing, media was removed carefully, without disturbing the cells and 3-(4,5-dimethylthiazol-2-yl)-2,5- diphenyltetrazolium bromide (MTT;

5mg/ml) was added. Mitochondrial succinate dehydrogenase reduces MTT to purple-coloured, water-insoluble formazan crystals. The plate was incubated in dark for 4h at 37°C. Resultant formazan crystals were dissolved in DMSO (150 µL/well) and kept for about 5 minutes till the crystals were completely dissolved. Absorbance was measured at 540 nm using Synergy HTX Multimode Reader.

6.5.2 Results and Discussion

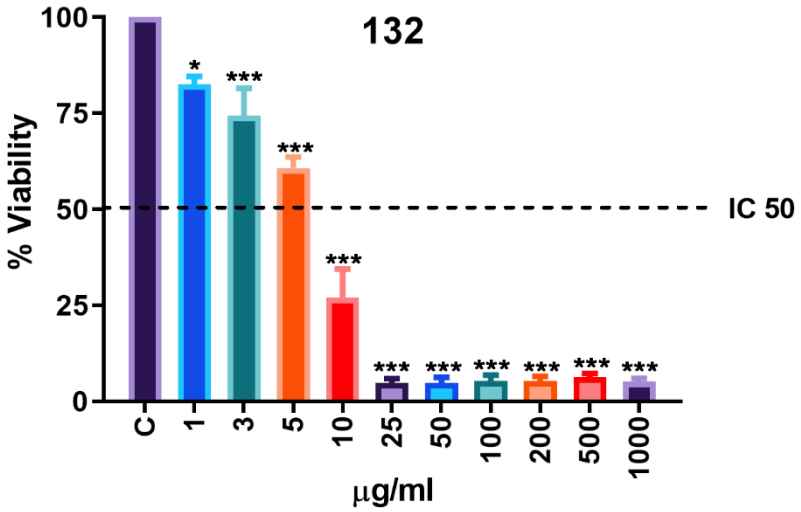

Figure 6.5.2.1 Cell viability verses concentration plots of **132** on human hepatoma (HepG2) cell line. Each point is the mean ± standard error obtained from three independent experiments.

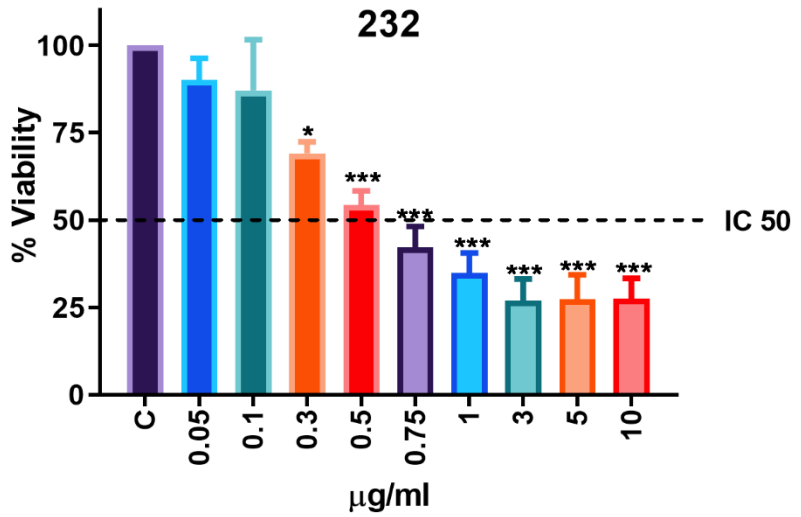

Figure 6.5.2.2 Cell viability verses concentration plots of **232** on human hepatoma (HepG2) cell line. Each point is the mean ± standard error obtained from three independent experiments.

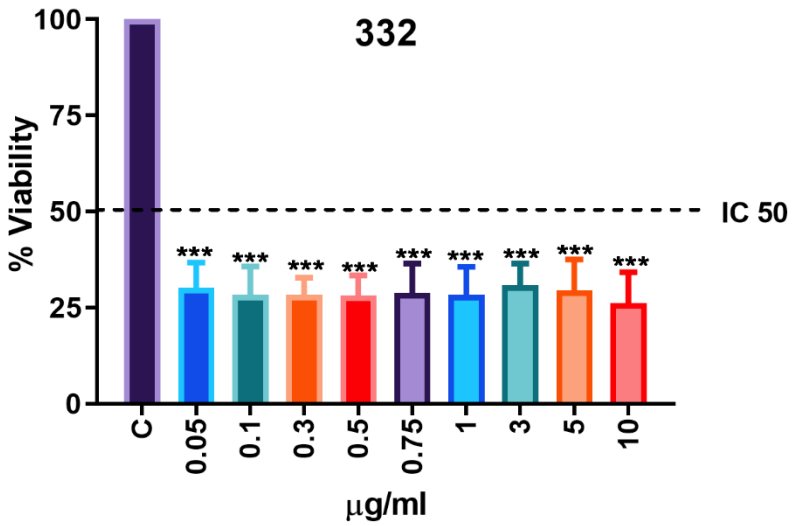

Figure 6.5.2.3 Cell viability verses concentration plots of **332** on human hepatoma (HepG2) cell line. Each point is the mean ± standard error obtained from three independent experiments.

In-vitro cytotoxicity tests of the trinuclear copper(II) metallogelator complexes were performed on the human hepatoma cancer cell line. The cell viabilities (%) were obtained with continuous exposure of the cells to the said complexes for 24 hours. The cytotoxicity of the complexes was found to be dose dependent, that is, the cell viability decreased with increasing concentrations **(Figure 6.5.2.1 to Figure 6.5.2.3)**. The inhibitory concentration 50 (IC_{50}), is defined as the concentration required to reduce the size of the cell population by 50%. The IC_{50} values of the complexes have been tabulated in **Table 6.5.2.1**. It is observed that the metallogelator complex **332** with neocuproine as the capping ligand **(IC_{50} = 0.03367 µg/mL)** is the most cytotoxic among all the various synthesized complexes. The metallogelator complexes **232** and **132** also exhibit low IC_{50} (µM) values of **0.6562 µg/mL** and **7.406 µg/mL** respectively.

The cytotoxicity of the complexes follows the order **332 > 232 > 132**. It was observed that when the capping ligands were changed from bipy to phen or neocuproine the cytotoxicity of the complexes increased.

It was also observed that the IC_{50} values of the metallogelator complexes are far lower (better cytotoxicity) as compared to copper(II) acetate which was used as a starting material for the preparation of these complex gelator molecules **(Table 6.5.2.1).** Such low IC_{50} values of the complexes can be attributed to 2 main reasons (i) high solubility of the complexes in water (being hydrogelator complexes) and (ii) presence of ligands capable of binding the DNA in intercalation mode, thus resulting in the cleavage and

cytotoxic property (especially in the case of complexes 232 and 332 having phen and neocuproine as capping ligands, respectively).

Table 6.5.2.1 IC_{50} values of complexes obtained from MTT assay on Human Hepatoma cell lines. Values have been expressed in **µg/mL.**

Codes	IC_{50} values
132	**7.406**
232	**0.6562**
332	**0.03367**
Copper(II) acetate	**25**

6.6 Antimicrobial analysis

Copper metal as mentioned earlier is one of the essential trace elements and a number of copper containing proteins have been known. The use of copper by human civilizations dates back to between the 5th and 6th millennia B.C. The Egyptians made use of copper to sterilize chest wounds and drinking water.[42] Greeks, Romans, Aztecs and others also used copper or copper compounds for the treatment of ailments as headaches, burns, intestinal worms, and ear infections and for hygiene in general. In the 19th century, a new awareness of copper's medical potency was given a rebirth by the observation that copper workers appeared to be resistant to cholera in the 1832 and subsequent outbreaks in Paris, France. The use of copper as an antimicrobial agent continued until the advent of commercially available antibiotics in 1932. While this approach is not novel,[42] it had lost importance and acceptance in the last few decades. A 1983 report documenting the beneficial effects of using brass and bronze on doorknobs to prevent the spread of microbes in a hospital remained largely unnoticed. Similarly, the idea of using copper vessels to render water drinkable has been revived only very recently as a low-cost alternative for developing countries. Currently, there is an intense interest in the use of copper as a self-sanitizing material, and many recent publications deal with mechanistic aspects of "contact killing" (contact-mediated killing) by copper.[42] Very obviously, complexes of copper are expected to possess antimicrobial activity.

The antimicrobial activity of the complexes was checked on 2 strains of gram positive ***(Staphylococcus aureus and Bacillus subtilis)*** and 2 strains of gram-negative bacteria ***(Pseudomonas aeruginosa and Escherichia coli)*** since the gels have copper in the

framework. Since the gels have an advantage of tropical application, this can have an added advantage over the conventional complexes if the gels can exhibit good antimicrobial properties.

6.6.1 Experimental Procedure

6.6.1.1 Antibacterial studies

The antimicrobial activity of the complexes was checked on 2 strains of gram positive ***(Staphylococcus aureus and Bacillus subtilis)*** and 2 strains of gram-negative bacteria ***(Pseudomonas aeruginosa and Escherichia coli)*****.** The bacterial culture was grown in a petri dish to which the complexes were added in different concentrations. Stock solutions of 1280 µg/mL of the complexes were prepared. Different concentrations of the complexes were added to the bacterial culture in the petri dish and were incubated for 24 hours, post which the zone of inhibition was checked to record the MIC (Minimum inhibitory concentration) of the complexes **(Figure 6.6.2.1 to Figure 6.6.2.5)**.

6.6.2 Results and Discussion

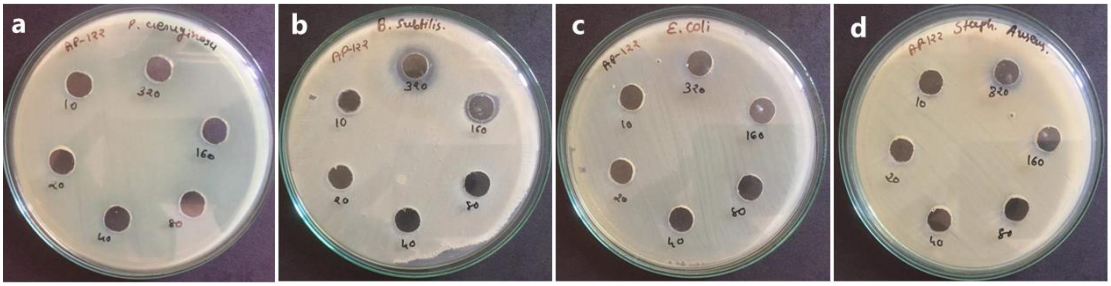

Figure 6.6.2.1 The bacterial culture medium for the activity of metallogel **122** against (a) Pseudomonas aeruginosa (b) Bacillus subtilis (c) Escherichia coli and (d) Staphylococcus aureus.

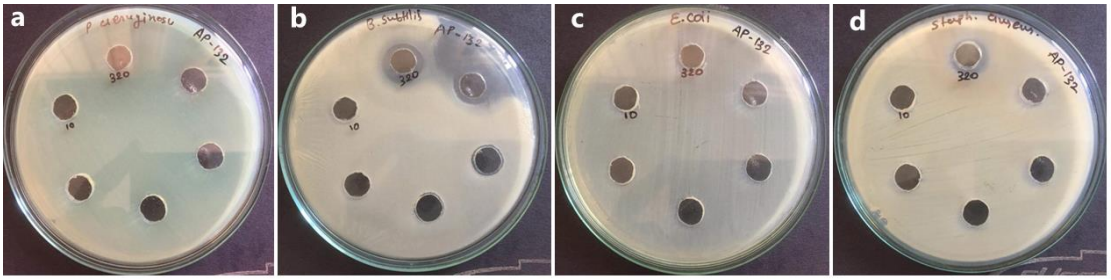

Figure 6.6.2.2 The bacterial culture medium for the activity of metallogel **132** against (a) Pseudomonas aeruginosa (b) Bacillus subtilis (c) Escherichia coli and (d) Staphylococcus aureus.

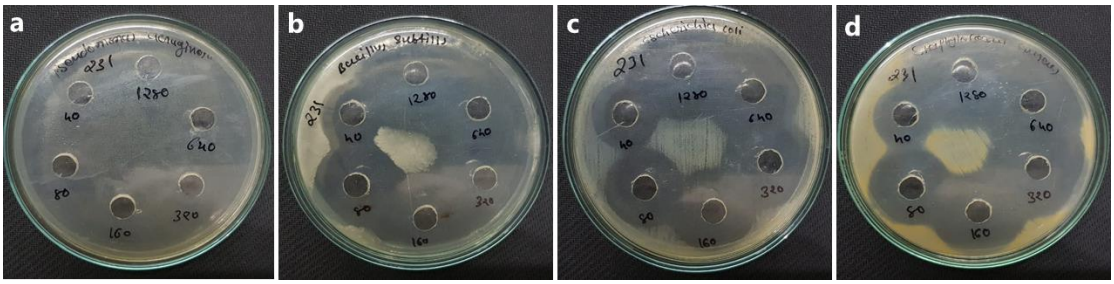

Figure 6.6.2.3 The bacterial culture medium for the activity of metallogel **231** against (a) Pseudomonas aeruginosa (b) Bacillus subtilis (c) Escherichia coli and (d) Staphylococcus aureus.

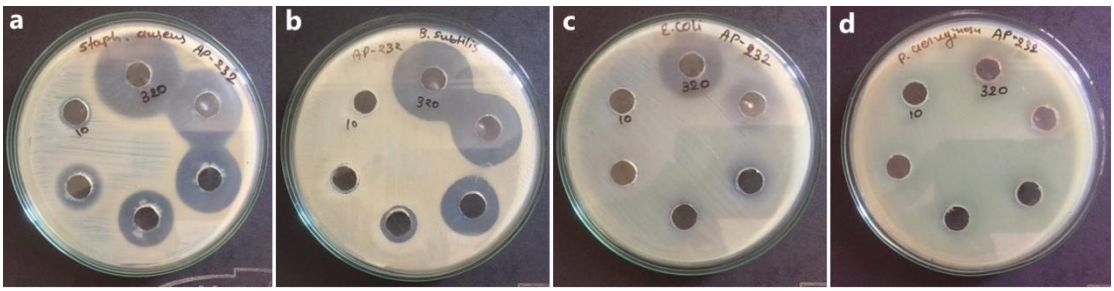

Figure 6.6.2.4 The bacterial culture medium for the activity of metallogel **232** against (a) Pseudomonas aeruginosa (b) Bacillus subtilis (c) Escherichia coli and (d) Staphylococcus aureus.

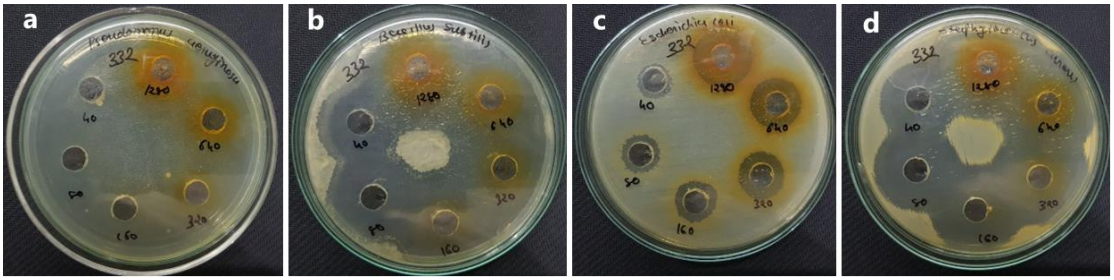

Figure 6.6.2.5 The bacterial culture medium for the activity of metallogel **332** against (a) Pseudomonas aeruginosa (b) Bacillus subtilis (c) Escherichia coli and (d) Staphylococcus aureus.

The minimum inhibitory concentrations of complexes were determined by liquid dilution method. The minimum inhibitory concentration at which no growth was observed was taken as the MIC values. The MIC values along with their activity against the 4 bacterial strains has been documented in the **Table 6.6.2.1 and Table 6.6.2.2.**

The series of metallogels having phen **(231 and 232)** and neocuproine **(332)** as the capping agents possessed good antibacterial activity against both gram-positive strains. They were also found to be active against gram negative bacterial strain ***Escherichia coli***. However, the activity was not that good as compared to gram positive strains. The higher antibacterial activity of the copper complexes is may be due to the change in structure due to coordination that tends to make metal complexes as more powerful and potent bacteriostatic agents, thus inhibiting the growth of the bacteria.

Table 6.6.2.1 The activity and MIC values of metallogels **122, 132** and **232** against gram positive and gram-negative bacterial strains

Code (Gel)	10 µg	20 µg	40 µg	80 µg	160 µg	320 µg	MIC
Escherichia coli (Gram -ve)							
122	10	10	10	10	10	10	>320 µg
132	10	10	10	10	10	10	>320 µg
232	10	10	10	**12**	**15**	**23**	**80**µg
Pseudomonas aeruginosa (Gram -ve)							
122	10	10	10	10	10	10	>320 µg
132	10	10	10	10	10	10	>320 µg
232	10	10	10	10	10	10	>320 µg
Staphylococcus aureus (Gram +ve)							
122	10	10	10	10	10	**11**	**320**µg
132	10	10	10	10	10	**13**	**320**µg
232	**11**	**16**	**21**	**25**	**29**	**32**	**10µg**
Bacillus subtilis (Gram +ve)							
122	10	10	10	10	**13**	**14**	**160** µg
132	10	10	10	**12**	**14**	**15**	**80**µg
232	10	**11**	**14**	**21**	**26**	**30**	**20**µg

Table 6.6.2.2 The activity and MIC values of metallogels **231** and **332** against gram positive and gram-negative bacterial strains

Code (Gel)	40 µg	80 µg	160 µg	320 µg	640 µg	1280 µg	MIC
Escherichia coli (Gram -ve)							
231	**24**	**28**	**30**	**35**	**40**	**44**	**<40 µg**
332	**13**	**15**	**17**	**18**	**20**	**23**	**<40 µg**
Pseudomonas aeruginosa (Gram -ve)							
231	10	10	10	**11**	**12**	**15**	80 µg
332	10	10	**11**	**12**	**13**	**13**	160 µg
Staphylococcus aureus (Gram +ve)							
231	**24**	**30**	**33**	**37**	**42**	**48**	**<40 µg**
332	**30**	**33**	**37**	**42**	**44**	**48**	**<40 µg**
Bacillus subtilis (Gram +ve)							
231	**23**	**30**	**33**	**37**	**42**	**48**	**<40 µg**
332	**30**	**35**	**44**	**48**	**48**	**48**	**<40 µg**

Table 6.6.2.3 The antibacterial values for Ciprofloxacin (Standard Antibacterial Agent)

CIPROFLOXACIN (Standard Antibacterial Agent)								
STRAIN	**5 µg**	**10 µg**	**15 µg**	**20 µg**	**30 µg**	**35 µg**	**40 µg**	**MIC**
Pseudomonas aeruginosa	12 mm	14 mm	16 mm	22 mm	30 mm	32 mm	35 mm	**05 µg**
Escherichia coli	10 mm	10 mm	12 mm	14 mm	17 mm	20 mm	24 mm	**15 µg**
Staphylococcus aureus	10 mm	10 mm	12 mm	15 mm	19 mm	23 mm	27 mm	**15 µg**
Bacillus subtilis	11 mm	13 mm	18 mm	19 mm	22 mm	25 mm	31 mm	**05 µg**

3 complexes out of 5 **(231, 232, and 332)** were very highly potent against both gram-positive strains. However, complexes containing bipy as the capping ligands were not very active against either of the strains. Thus, the change in the structure of the coordination sphere appears to play a significant role in deciding the antibacterial activity of the complexes. The gram-positive bacteria were much more susceptible to the metallogelator complexes as compared to gram-negative bacteria. The metallogelator complexes were also compared with a commercial antibiotic, Ciprofloxacin, which was used as a standard/reference molecule. The metallogelator complex **232** showed very good activity against grampositive bacteria and lower MIC against ***Staphylococcus aureusas*** compared to the standard Ciprofloxacin drug **(Table 6.6.2.3)**. The same complex also showed fairly good activity against gram positive bacteria ***Bacillus subtilis*** with the MIC value of 20 µg. However, the MIC of **232** was higher as compared to Ciprofloxacin (5 µg) for the ***Bacillus subtilis*** strain. These being gel forming complexes, incorporation of suitable drug molecules in the gel can be further enhance their efficacy and indicate the possibility of combination therapy.

6.7 Conclusions

- All the gel-forming copper(II) complexes synthesized turned out to be catalytically active SOD mimics, being able to scavenge the superoxide radical at exceptionally low concentrations.
- The SOD values of the metallogels depend on the capping agent, counter anion and the base used for gelation.
- UV-Vis spectroscopy and fluorescence studies show that the gels having phenanthroline and neocuproine as capping ligands have strong binding with DNA and BSA.
- The cytotoxicity studies on human hepatoma cell line shows that the metallogelator complexes especially **232** and **332** have excellent cytotoxicity and very low IC_{50} values.
- The gels having phenanthroline and neocuproine as capping agents also show very good activity against gram positive bacteria and have lower MIC against Staphylococcus aureus as compared to the standard antibiotic, Ciprofloxacin.

REFERENCES

1. Wood, J. M. Biological Cycles for Elements in the Environment. *Naturwissenschaften* **62**, 357–364 (1975).
2. Uhlenheuer, D. A., Petkau, K. & Brunsveld, L. Combining supramolecular chemistry with biology. *Chem. Soc. Rev.* **39**, 2817–2826 (2010).
3. Metcalfe, C. & Thomas, J. A. Kinetically inert transition metal complexes that reversibly bind to DNA. *Chem. Soc. Rev.* **32**, 215–224 (2003).
4. Krishnamoorthy, P., Sathyadevi, P., Cowley, A. H., Butorac, R. R. & Dharmaraj, N. Evaluation of DNA binding, DNA cleavage, protein binding and in vitro cytotoxic activities of bivalent transition metal hydrazone complexes. *Eur. J. Med. Chem.* **46**, 3376–3387 (2011).
5. Kellett, A., Molphy, Z., Slator, C., Mckee, V. & Farrell, N. P. Molecular methods for assessment of non-covalent metallodrug–DNA interactions. *Chem. Soc. Rev.* **48**, 971–988 (2019).
6. Pyle, A. M. Rehmann, J. P. Meshoyrer, R. Kumar, C. V. Turro, N. J. Barton, J. K. Mixed-Ligand Complexes of Ruthenium(II): Factors Governing Binding to DNA. *J. Am. Chem. Soc.* **111**, 3051–3058 (1989).
7. Xiang, Y. & Wu, F. Study of the interaction between a new Schiff-base complex and bovine serum albumin by fluorescence spectroscopy. *Spectrochim. Acta. A. Mol. Biomol. Spectrosc.* **77**, 430–436 (2010).
8. Theodore Peters, J. *All About Albumin - Biochemistry, Genetics, and Medical Applications*. (Elsevier Inc., 1995).
9. Zhou, X.-Q. Sun, Q. Jiang, L. Li, S.-T. Gu, W. Tian, J.-L. Liu, X. Yan, S.-P. Synthesis, Characterization, DNA/BSA interactions and Anticancer Activity of achiral and chiral copper complexes. *Dalt. Trans.* **44**, 9516–9527 (2015).
10. Lakowicz, J. R. & Weber, G. Quenching of fluorescence by oxygen. A probe for structural fluctuations in macromolecules. *Biochemistry* **12**, 4161–4170 (1973).
11. Min, J., Meng-Xia, X., Dong, Z., Yuan, L., Xiao-Yu, L. & Xing, C. Spectroscopic studies on the interaction of cinnamic acid and its hydroxyl derivatives with human serum albumin. *J. Mol. Struct.* **692**, 71–80 (2004).
12. Shahabadi, N. & Mohammadpur, M. Study on the interaction of sodium morin-5-sulfonate with bovine serum albumin by spectroscopic techniques. *Spectrochim. Acta Part A Mol. Biomol. Spectrosc.* **86**, 191–195 (2012).
13. Tang, J., Luan, F. & Chen, X. Binding analysis of glycyrrhetinic acid to human serum albumin: Fluorescence spectroscopy, FTIR, and molecular modeling. *Bioorganic Med. Chem.* **14**, 3210–3217 (2006).
14. Senthil Raja, D., Bhuvanesh, N. S. P. & Natarajan, K. Effect of N(4)-phenyl substitution in 2-oxo-1,2-dihydroquinoline-3- carbaldehyde semicarbazones on the structure, DNA/protein interaction, and antioxidative and cytotoxic activity of Cu(II) complexes. *Inorg. Chem.* **50**, 12852–12866 (2011).
15. Riley, D. P. Functional Mimics of Superoxide Dismutase Enzymes as Therapeutic Agents. *Chem. Rev.* **99**, 2573–2587 (1999).
16. Sheng, Y., Abreu, I. A., Cabelli, D. E., Maroney, M. J., Miller, A. F., Teixeira,

M. & Valentine, J. S. Superoxide dismutases and superoxide reductases. *Chem. Rev.* **114**, 3854–3918 (2014).

17. Sankaralingam, M., Lee, Y. M., Nam, W. & Fukuzumi, S. Amphoteric reactivity of metal–oxygen complexes in oxidation reactions. *Coord. Chem. Rev.* **365**, 41–59 (2018).
18. Fukuzumi, S., Ohtsu, H., Ohkubo, K., Itoh, S. & Imahori, H. Formation of superoxide-metal ion complexes and the electron transfer catalysis. *Coord. Chem. Rev.* **226**, 71–80 (2002).
19. Fukuzumi, S., Lee, Y. M. & Nam, W. Structure and reactivity of the first-row d-block metal-superoxo complexes. *Dalt. Trans.* **48**, 9469–9489 (2019).
20. Balasubramanian, V., Ezhevskaya, M., Moons, H., Markus Neuburger, Carol Cristescu, S. V. D. & Cornelia, P. Structural characterization of a highly active superoxide-dismutase mimic. *Phys. Chem. Chem. Phys.* **11**, 6778–6787 (2009).
21. Potapov, A. S., Nudnova, E. A., Domina, G. A., Kirpotina, L. N., Quinn, M. T., Khlebnikov, A. I. & Schepetkin, I. A. Synthesis, characterization and potent superoxide dismutase-like activity of novel bis(pyrazole)-2,2′-bipyridyl mixed ligand copper(II) complexes. *Dalt. Trans.* 4488–4498 (2009).
22. Anacona, J. R., Gutierrez, C. & Rodriguez-Barbarin, C. Crystal structure and superoxide dismutase activity of [Cu(ethylenediamine)2Cl] [PF6]. *Monatshefte fur Chemie* **135**, 785–792 (2004).
23. Weser, U. & Schubotz, L. M. Imidazole-bridged copper complexes as Cu2Zn2-Superoxide dismutase models. *J. Mol. Catal.* **13**, 249–261 (1981).
24. Li, Y., Yang, Z. Y. & Wu, J. C. Synthesis, crystal structures, biological activities and fluorescence studies of transition metal complexes with 3-carbaldehyde chromone thiosemicarbazone. *Eur. J. Med. Chem.* **45**, 5692–5701 (2010).
25. Terra, W. S., Ferreira, S. S., Costa, R. O., Mendes, L. L., Franco, R. W. A., Bortoluzzi, A. J., Resende, J. A. L. C., Fernandes, C. & Horn, A. Evaluating the influence of the diamine unit (ethylenediamine, piperazine and homopiperazine) on the molecular structure, physical chemical properties and superoxide dismutase activity of copper complexes. *Inorganica Chim. Acta* **450**, 353–363 (2016).
26. O'Connor, M., Kellett, A., McCann, M., Rosair, G., McNamara, M., Howe, O., Creaven, B. S., McClean, S., Foltyn-Arfa Kia, A., O'Shea, D. & Devereux, M. Copper(II) complexes of salicylic acid combining superoxide dismutase mimetic properties with DNA binding and cleaving capabilities display promising chemotherapeutic potential with fast acting in vitro cytotoxicity against cisplatin sensitive and resista. *J. Med. Chem.* **55**, 1957–1968 (2012).
27. Roy, S., Banerjee, A., Lima, S., Horn, A., Sampaio, R. M. S. N., Ribeiro, N., Correia, I., Avecilla, F., Carvalho, M. F. N. N., Kuznetsov, M. L., Pessoa, J. C., Kaminsky, W. & Dinda, R. Unusual chemistry of Cu(ii) salan complexes: Synthesis, characterization and superoxide dismutase activity. *New J. Chem.* **44**, 11457–11470 (2020).
28. Reddy, K. S. Global Burden of Disease Study 2015 provides GPS for global health 2030. *Lancet* **388**, 1448–1449 (2016).

29. Liu, H., Chen, L., Xu, C., Li, Z. & Zhang, H. Chem Soc Rev Recent progresses in small-molecule enzymatic. *Chem. Soc. Rev.* **47**, 7140–7180 (2018).
30. Rosenberg B., VanCamp L., Trosko J.E., M. V. H. Platinum compounds: A new class of potent antitumour agents. *Nature* **222**, 385–386 (1969).
31. Alderden, R. a, Hall, M. D. & Hambley, T. W. Products of Chemistry The Discovery and Development of Cisplatin. *J. Chem. Educ.* **83**, 728–734 (2006).
32. Dilruba, S. & Kalayda, G. V. Platinum-based drugs: past, present and future. *Cancer Chemother. Pharmacol.* **77**, 1103–1124 (2016).
33. Herradón, E., González, C., Uranga, J. A., Abalo, R., Martín, M. I. & López-Miranda, V. Characterization of cardiovascular alterations induced by different chronic cisplatin treatments. *Front. Pharmacol.* **8**, 1–15 (2017).
34. Manohar, S. & Leung, N. Cisplatin nephrotoxicity: a review of the literature. *J. Nephrol.* **31**, 15–25 (2018).
35. Dasari, S. & Bernard Tchounwou, P. Cisplatin in cancer therapy: Molecular mechanisms of action. *Eur. J. Pharmacol.* **740**, 364–378 (2014).
36. Komeda, S. & Casini, A. Next-Generation Anticancer Metallodrugs. *Curr. Top. Med. Chem.* **12**, 219–235 (2012).
37. Zeng, L., Gupta, P., Chen, Y., Wang, E., Ji, L., Chao, H. & Chen, Z. S. The development of anticancer ruthenium(II) complexes: From single molecule compounds to nanomaterials. *Chem. Soc. Rev.* **46**, 5771–5804 (2017).
38. Tardito, S. & Marchio, L. Copper Compounds in Anticancer Strategies. *Curr. Med. Chem.* **16**, 1325–1348 (2009).
39. Jungwirth, U., Kowol, C. R., Keppler, B. K., Hartinger, C. G., Berger, W. & Heffeter, P. Anticancer activity of metal complexes: Involvement of redox processes. *Antioxidants Redox Signal.* **15**, 1085–1127 (2011).
40. Santini, C., Pellei, M., Gandin, V., Porchia, M., Tisato, F. & Marzano, C. Advances in copper complexes as anticancer agents. *Chem. Rev.* **114**, 815–862 (2014).
41. Marzano, C., Pellei, M., Tisato, F. & Santini, C. Copper Complexes as Anticancer Agents. *Anticancer. Agents Med. Chem.* **9**, 185–211 (2012).
42. Grass, G., Rensing, C. & Solioz, M. Metallic Copper as an Antimicrobial Surface. *Appl. Environ. Microbiol.* **77**, 1541–1547 (2010).

•